Protein-based artificial retinas

Zhongping Chen and Robert R. Birge

Artificial retinas based on the light transducing photoelectric protein bacteriorhodopsin exhibit differential responsivity, edge enhancement and motion detection. Under appropriate conditions, these artificial receptors mimic the differential responsivity characteristic of mammalian photoreceptor cells. The use of orientated bacteriorhodopsin to generate the photoelectrical signal provides rapid responsivity, high quantum efficiency and offers the potential of directly coupling the protein response to charge-sensitive semiconductor arrays. The ability to manipulate the properties of the protein via chemical and genetic methods enhances design flexibility.

The eye provides the single most important sensor with which higher animals and humans perceive the world. The amount of information that the human visual system must receive and process in real time is many orders of magnitude larger than that required for the other senses, such as smell and hearing. Accordingly, a significant portion of the brain is allocated to visual processing. The sophistication of the visual cortex notwithstanding, evolution has developed a considerable pre-processing capability within the neural system of the eye to optimize the information content of the signal transferred along the optic nerve. The processing capability of the human retina far outstrips that of the most powerful supercomputers[1]. Efforts to model the retina by using semiconductor circuitry have been partially successful[1], but the complexity of such circuitry precludes the full implementation of many processing functions inherent in the biological retina. Furthermore, the resolution is significantly lower than that achieved by the biological retina. Biotechnology may offer new ways to generate artificial retinas, and this review examines current efforts to create artificial retinas based on the use of the photoelectric protein, bacteriorhodopsin. This protein has a number of intrinsic photochemical and photoelectric properties that are well suited to exploitation in artificial retinas. In addition, the potential for enhancing the functionality of the protein by using chemical and genetic manipulation provides an additional avenue for optimization that is unique to protein-based designs.

After reviewing the principal photochemical properties of bacteriorhodopsin and the key features of the pre-processing functions of vertebrate retinas, we examine current photoreceptor imaging systems that are based on bacteriorhodopsin and that provide partial pre-processing capability. The development of artificial retinas based on bacteriorhodopsin is in the early stages of research, and much remains to be accomplished. Nevertheless, the demonstration of differential responsivity inherent in oriented thin films of this protein has already yielded edge-enhancement and motion-detection capabilities that are unique and promising.

Z. Chen and R. R. Birge are at the W. M. Keck Center for Molecular Electronics, Syracuse University and Biological Components Corporation, Syracuse, NY 13244-4100, USA.

Photophysical properties of bacteriorhodopsin

Bacteriorhodopsin (MW ≅ 26000) is the light-harvesting protein in the purple membrane of a microorganism called *Halobacterium halobium*[2,3]. The bacterium grows in salt marshes where the concentration of salt is roughly six times higher than that of sea water. The purple membrane develops when the concentration of oxygen becomes too low to sustain respiration. The protein, upon the absorption of light, pumps a proton across the membrane, generating a chemical and osmotic potential that serves as an alternative source of energy. Thus, *Halobacterium halobium* can switch from respiration to photosynthesis when the need arises. The fact that the protein must survive in the harsh environment of a salt marsh, where the temperatures can exceed 65°C for extended periods of time, requires a robust protein that is resistant to thermal and photochemical damage. While *in vivo* stability does not always translate into *in vitro* stability, excellent stability is observed in the case of bacteriorhodopsin, provided that the purple membrane fragments are not sonicated so as to destroy the protein trimeric arrangement. The cyclicity of the protein (i.e. the number of times it can be photochemically cycled) exceeds 10^6, a value considerably higher than most synthetic photochromic materials. Thus, the common perception that biological materials cannot be used in devices because they are too fragile does not apply to bacteriorhodopsin. The key characteristics of bacteriorhodopsin that are relevant to the performance of this protein in optoelectronic devices are shown in Table 1.

 0167 - 7799/93/$6.00

Table 1. Properties and characteristics of bacteriorhodopsin (bR) and bacteriorhodopsin-based materials[a]

Property	Description	Values
Molecular weight and structure	Membrane-bound protein with 248 amino acids arranged in 7 α-helical segments; purple membrane patch (10 lipid molecules per protein; 40 nm x 500 nm x 500 nm) is a two-dimensional crystalline lattice consisting of trimers	MW ≅ 26 000 Da
Chromophore	Protonated Schiff base of all-*trans* retinal, attached via lysine-216, embedded inside highly polar binding site	MW ≅ 280 Da
Biological function	Light-driven proton pump used by bacterium as a source of energy when low oxygen level prevents respiration	
Stability[b]	Protein can withstand constant illumination, oxygen, pH 3–10, temperatures below 80°C, most hydrophilic polymers	$3 < pH < 10$ $T < 80°C$
Instabilities	UV irradiation ($\lambda < 370$ nm), most organic solvents, pH extremes	$\lambda < 370$ nm
Photochemistry	Absorption of light generates photocycle via *cis–trans* isomerization of the chromophore; high quantum efficiency	$\Phi \cong 0.65$
Wavelength range	Range of activation wavelength extends throughout visible region of the spectrum (values in nanometers); chromophore analogs can extend range	$400 < \lambda < 660$
Resolution	Diffraction-limited performance is typical	5000 lines mm^{-1}
Diffraction efficiency	Holographic performance for absorption holograms is absorption-limited (< 3.7%); phase performance is better	$\eta_{abs} \leq 3.7\%$ $\eta_{phase} \leq 8\%$
Reversibility	The protein is photochemically robust due to protective characteristics of the protein-binding site; cyclicity (total number of write, read, erase cycles) is excellent	Cyclicity $\geq 10^6$
Sensitivity	Sensitivity can be optimized for specific application	1–80 mJ cm^{-2}
Thin films	Thin films can be prepared with diffraction-limited optical properties using hydrophilic gels, polymers and blends	Thickness = 20–500 μm
Relaxation time	Thermal relaxation time of the blue intermediate (M) can be varied from 10 ms to infinity and is affected by pH, chemical environment, site-specific mutation and temperature	τ_T variable $\tau_{h\nu} \leq 50$ μs
One-photon absorptivity	Values for the molar absorptivity at λ_{max} in units of M^{-1} cm^{-1} are given for bR (λ_{max} = 570 nm) and M (λ_{max} = 410 nm)	$\epsilon_{bR} \cong 66{,}000$ $\epsilon_M \cong 45{,}000$

[a]Data collected from Refs 3–5.
[b]Stability is a time- and temperature-dependent property. As the temperature approaches 80°C, denaturation is fairly rapid, photochemical stability decreases and pH sensitivity increases. The protein trimer is much more stable than the monomer.

The light-absorbing chromophore of bacteriorhodopsin is all-*trans* retinal (vitamin A aldehyde). It is bound to the protein via a protonated linkage to a lysine residue attached to the protein backbone (Fig. 1). The bound chromophore carries a positive charge, which interacts electrostatically with charged amino acids in the protein-binding site. These interactions impart photochemical properties to the chromophore that differ significantly from those observed for the chromophore in solution. When the protein absorbs light in the native organism, it undergoes a complex photocycle that generates intermediates with absorption maxima spanning the entire visible region of the spectrum (Fig. 2). Many of the early optical devices based on bacteriorhodopsin operated at liquid-nitrogen temperature and used photochemical switching between the light-activated bacteriorhodopsin (bR) and the intermediate K states[10]. While these devices were efficient and potentially very fast (the bR ⇔ K interconversions take place in a few picoseconds), the use of cryogenic temperatures precluded general application. The artificial retinas described in this study operate at ambient temperature and use the following two states: the initial green absorbing state (bR) and

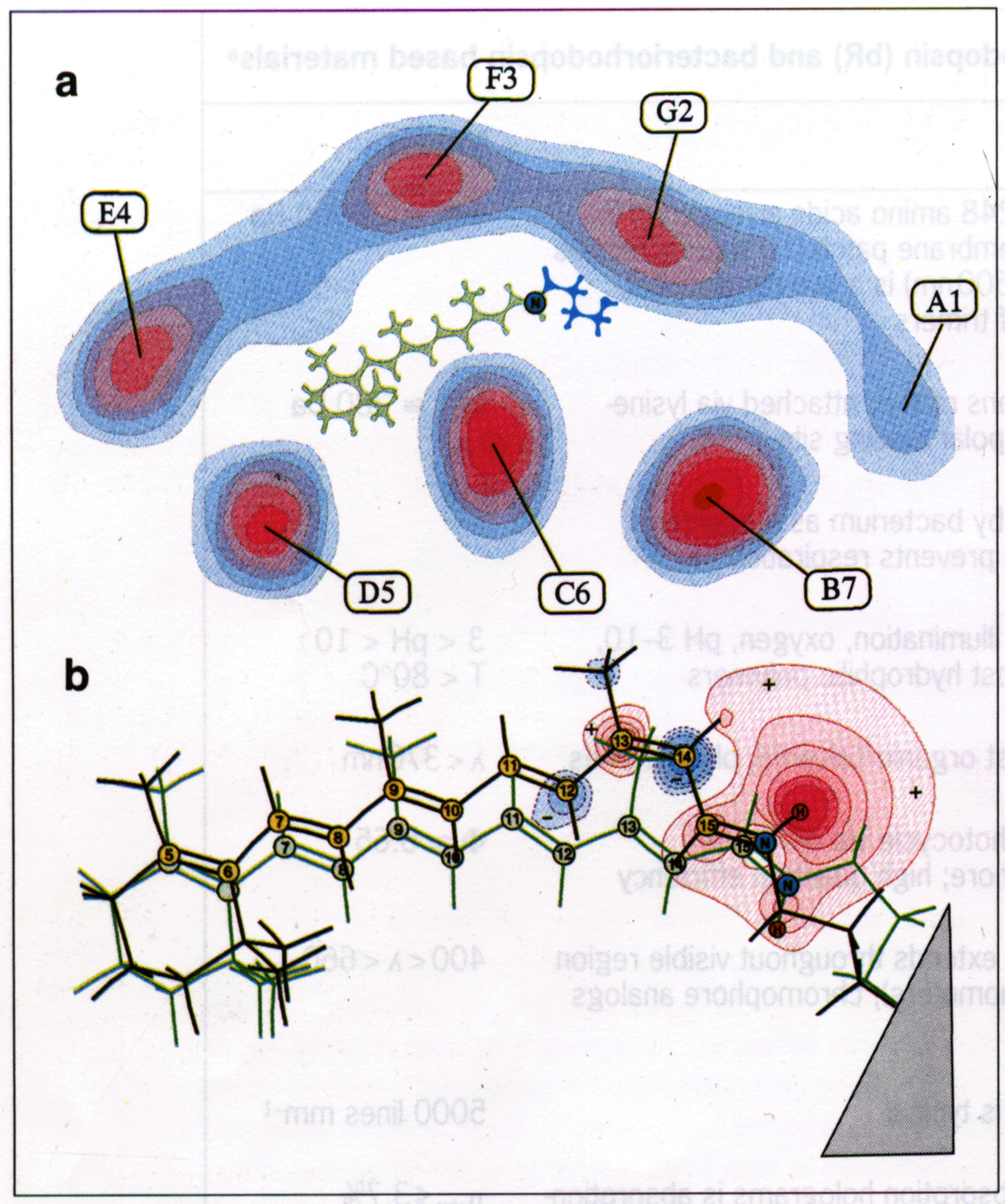

Figure 1

The chromophore-binding site and the primary photochemical event in bacteriorhodopsin. (**a**) Electron-density profiles (data from Ref. 6) of bacteriorhodopsin viewed from the cytoplasmic side, showing the seven transmembrane-spanning segments and the presumed location of the chromophore in relation to the helices, based on the available experimental data[3,7,8]. Fourier-transform infrared spectroscopy studies indicate that the polyene chain of the chromophore in bacteriorhodopsin lies roughly perpendicular to the membrane plane[9]. The retinyl chromophore is rotated artificially into the membrane plane to show more clearly the polyene chain (the imine nitrogen is indicated by a solid black circle) and the β-ionylidene ring. (**b**) A model of the primary photochemical event [light-adapted bacteriorhodopsin (bR) (gray; underneath) → K (black; above)] and the shift in charge that is associated with the motion of the positively charged chromophore following 13-*trans* → 13-*cis* photoisomerization. It is believed that the initial photoelectric signal is due primarily to the motion of the chromophore.

the long-lived blue absorbing state (M). The photochemistry is summarized below:

$$\begin{aligned} &\text{bR } (\lambda_{max} \cong 570\,\text{nm}) \text{ (\textit{State 0})} \\ &\Phi_1 \cong 0.65 \Downarrow \Uparrow \Phi_2 > 0.65 \\ &\text{M } (\lambda_{max} \cong 410\,\text{nm}) \text{ (\textit{State 1})} \end{aligned} \qquad (1)$$

The quantum efficiency of the forward reaction is indicated by Φ_1 and the quantum efficiency of the reverse reaction is indicated by Φ_2. The forward quantum efficiency is now well established experimentally ($\Phi_1 = 0.65 \pm 0.05$) (Ref. 4). The value for Φ_2 is less certain, but a majority of experimental measurements support the assumption that $\Phi_2 > \Phi_1$ (see discussion in Refs 3,4,7 and 8), and this is what we have indicated in Eqn 1. One of the important attributes of bacteriorhodopsin that is relevant to the use of this protein in artificial retinas is the high efficiency with which the protein converts light into a change in protein conformation and the photovoltaic signal that is thereby generated[4,7,8].

As noted above and in Table 1, the intrinsic properties of the native bacteriorhodopsin protein make it an outstanding candidate for use in photovoltaic imaging devices. The following list summarizes the key advantages that are particularly relevant to artificial retinas:

- long-term stability of the protein to thermal and photochemical degradation;

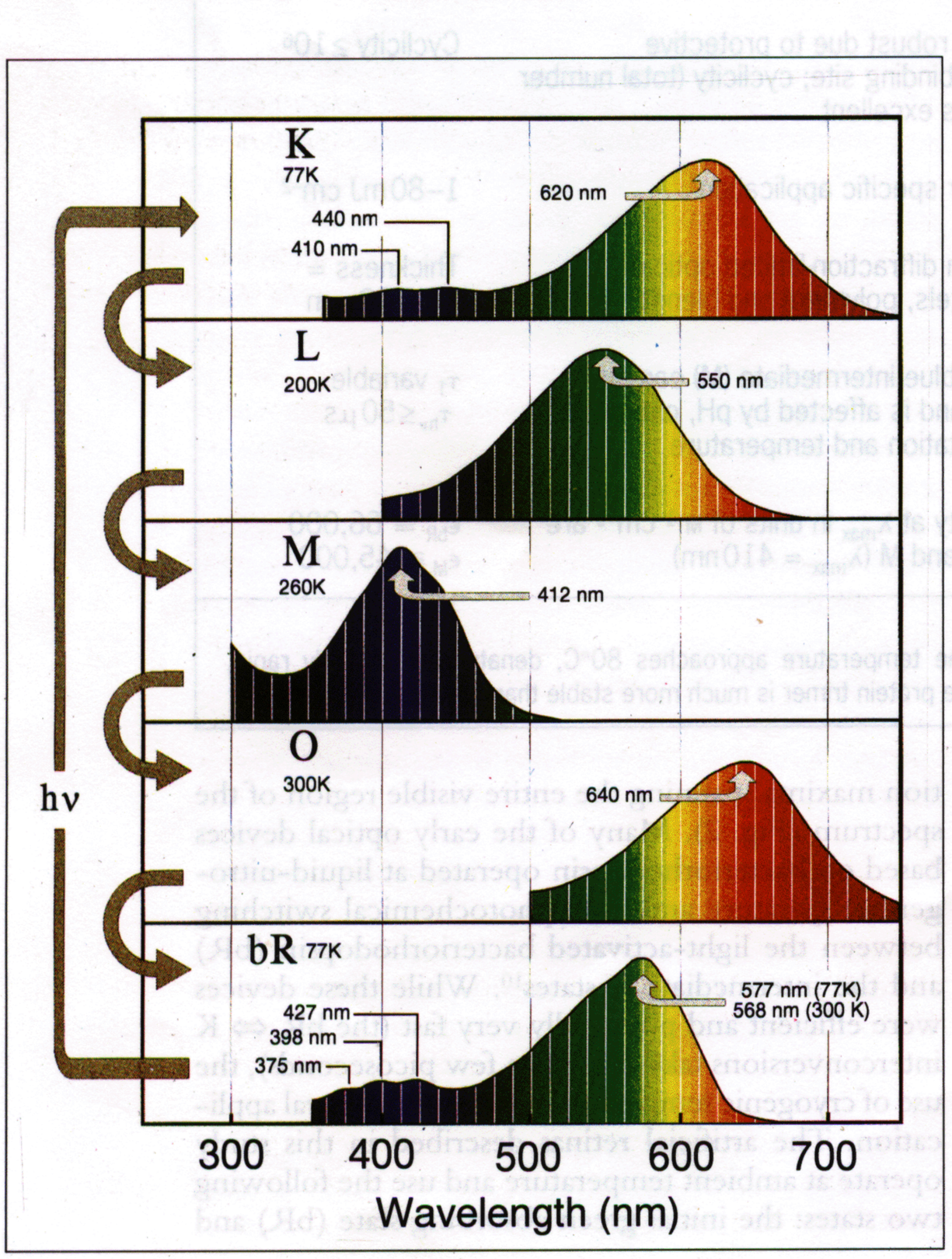

Figure 2

Photocycle of light-adapted bacteriorhodopsin (**bR**) showing the electronic (one-photon) absorption spectra of selected intermediates. Under ambient conditions, the only species that is stable indefinitely is bR. Upon absorption of light, bR converts to K which, at temperatures above 150K, converts in about 2 μs to L. This intermediate forms M in about 50 μs. At temperatures above 240K, M forms O in about 1 ms, and O converts to bR in about 10 ms. The rate of the M → O transition can be adjusted by changing temperature or by altering the chromophore (see text). Most devices operate by photochemically interconverting bR and M. The temperatures used to measure the spectra are indicated next to the intermediate labels. (Adapted from Refs 7,8.)

- high forward and reverse quantum yields, permitting the use of low light levels for activation;
- wavelength-independent quantum yields that permit flexibility in optical design;
- the generation of a photoelectric signal that has a different polarity for the forward compared with the reverse photoreaction (Eqn 1);
- a differential responsivity under certain conditions that mimic *in vivo* photoreceptors;
- a diffraction-limited performance due to the small size of the protein (50nm), relative to the wavelength of light (>400nm) and;
- the ability to form thin films or orientated polymer cubes containing bacteriorhodopsin with excellent optical properties.

The above properties can be enhanced selectively for specific applications by using chemical additives, substitution of different chromophores, or by changing the amino acid composition of the protein through genetic engineering. These techniques, as well as the use of bacteriorhodopsin in device applications, have been reviewed in detail recently[4,7,8].

Pre-processing in vertebrate retinas

Our goal is to mimic the pre-processing capabilities of mammalian retinas. It is therefore important to examine these capabilities in order to appreciate the goals that must be met to create artificial retinas. One of the key characteristics of the vertebrate visual system is the extensive processing of image data that occurs in the neural system in the back of the eye. Contrary to common belief, the optical signal that is transferred along the optic nerve is not a direct representation of the image imposed on the retina, but is modified and condensed based on image and motion content. The visual cortex in the brain actually processes only a small fraction of the image information relative to what would be necessary if no pre-filtering and discrimination were to take place in the neural system of the eye. Thus, the visual system actually involves two processing centers. The first is in the neural system in the back of the eye and the second is within the visual cortex of the brain. The two key visual processing capabilities inherent in the retina are edge discrimination and motion detection. These two capabilities are closely linked, and are often grouped using the term 'differential responsivity'. Differential responsivity results in a maximum signal amplitude from those receptor cells for which there is a large difference in light intensity relative to neighboring rod cells. Thus, the information transferred through the neural network is 'edge enhanced'.

A secondary attribute that is characteristic of the retina is to enhance image segments that are rapidly changing. Thus, the derivative of light intensity as a function of time is more important than the actual intensity of the light in determining whether a neural impulse is sent to the brain. These two characteristics are significantly different from the characteristics of standard semiconductor or vidicon imaging systems. Implementation of these characteristics within the front-end matrix of semiconductor imaging systems is both complicated and deleterious to resolution[1].

A detailed discussion of the structure and function of the retina is beyond the scope of this review, but relevant background reviews are Refs 1 and 11. Our discussion is restricted to an examination of the distribution of sensitivity within the receptive field of a ganglion cell with a plain receptive field (see Glossary). Such cells represent the commonest type of retina cell found in higher mammals, and a close look at their function provides an insight into how nature achieves the differential responsivity that is responsible for motion detection and edge enhancement. We will call this type of receptor ensemble an 'X-cell', a label derived from the extensive studies of the cat retina[11]. The response characteristics of the X-cell are shown in one-dimensional and two-dimensional plots in Fig. 3. The X-cell is characterized by a central excitatory region surrounded by a larger inhibitory region. The response characteristics are well described as a function of the second derivative of a Gaussian, and

Glossary

Difference-of-Gaussians (DOG) function – The DOG function is a convenient mathematical representation of the complex behavior of an X-type photoreceptor cell. By adding two such distributions with equal areas and centers consisting of a positive sharp one and a negative broader one .the DOG function described mathematically in Eqn 2 is achieved. Near the center of this distribution, the sharper distribution dominates and 'excitation' occurs. Away from the center the broader distribution dominates and 'inhibition' occurs. The DOG function is a good approximation to the spatial second derivative of a Gaussian distribution. Thus, if the DOG function is integrated over all space the result is zero (neither excitation nor inhibition). This mimics the response of an X-type cell.

Receptive field – The vertebrate retina consists of a number of laterally interconnected layers of cells through which information is preprocessed. A visual neuron responds to light excitation of the photoreceptors with characteristics that are both space and time dependent. The term receptive field describes the spatial–temporal relationship between the response of a neuron and the stimulation of the photoreceptor.

Plain receptive field – A plain receptive field is a receptive field possessing a linear response to light. The response of a neuron with a plain receptive field to a group of individual photoreceptor stimuli is equivalent to the response given by the sum of the individual stimuli presented separately. An example of a plain receptive field is that of the X-cell shown in Fig. 3b.

Retinal ganglion cell – The final layer of cells in retinal processing. The axons of these cells exit the retina through the so-called blind spot to form the optic nerve.

X-cell – One class of retinal ganglion cells. The receptive field of an X-cell consists of a central excitatory region surrounded by a larger inhibitory region. The X-cell response profile can be approximated by a Difference-of-Gaussians function (see Fig. 3a).

Edge enhancement – Any operation that enhances the contrast and increases the relative intensity of the edges (boundaries) of an object.

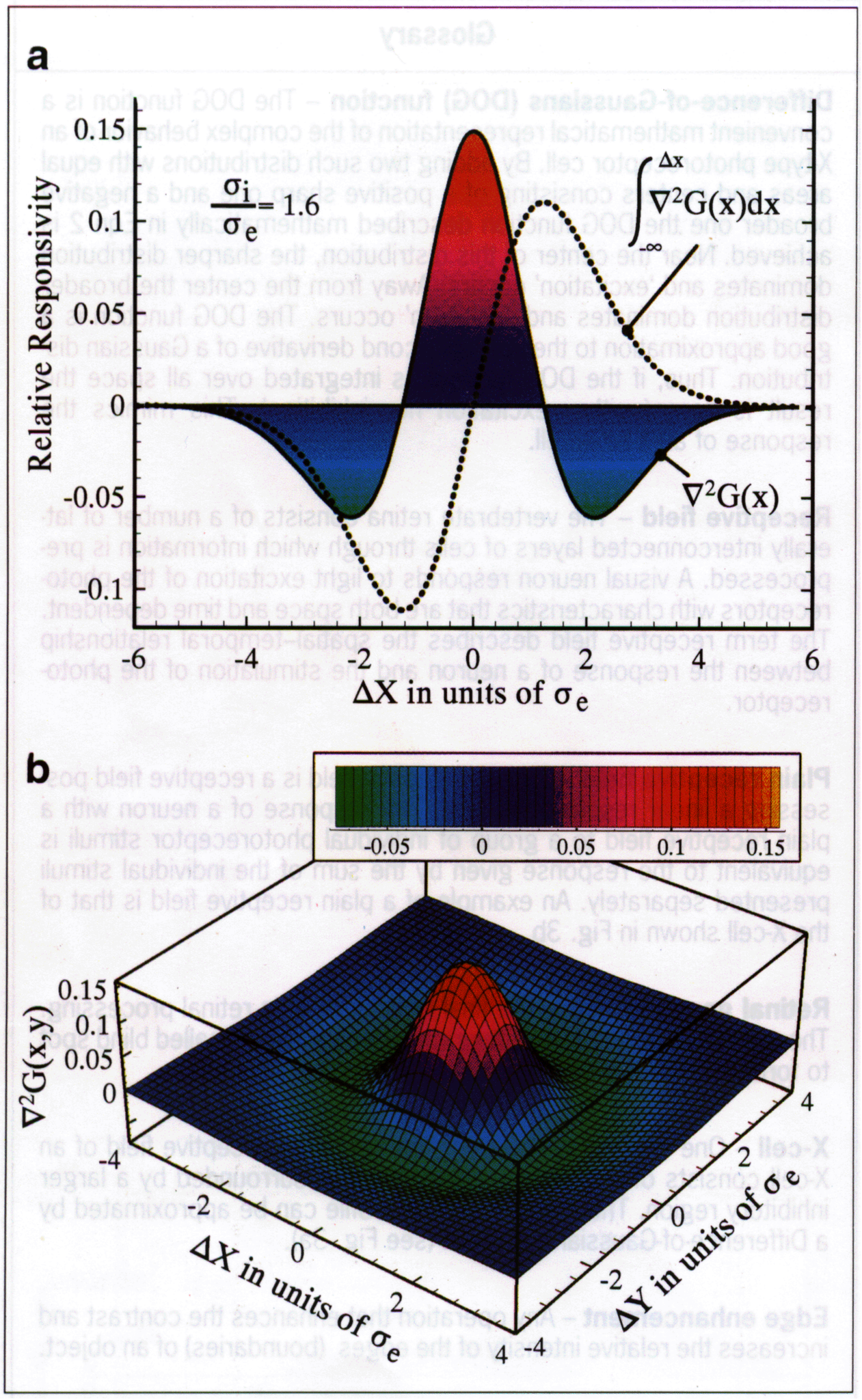

Figure 3

Simulation of (**a**) the one-dimensional and (**b**) two-dimensional response characteristics of a nominal X-type ganglion receptor cell. Regions of excitatory response are positive (dark blue, yellow to red) and regions of inhibitory response are negative (dark blue to light blue), and the relative responsivity is calculated by using the difference-of-Gaussians (DOG) approximation (Eqn 1). The dotted line in (**a**) shows the X-cell response for a constant-intensity, homogeneous light source illuminating from the far edge to a specified location (Δx) relative to the cell center. This response is equivalent to the integral of $\nabla^2 G(x)$ from $-\infty$ to Δx. If receptive fields are described by the second derivative of a Gaussian function, transformation carried out by projection of an image on the receptive fields is equal to taking the second derivative of the image after the image has been smoothed by a Gaussian filter, or equivalently, a convolution of the image with the receptive fields represented by the $\nabla^2 G$ profile. Such a receptive field is capable of locating a sharp spatial variation or edge in the image as illustrated in the one-dimensional plot shown in (**a**). The response of the receptive field to an edge intensity profile is shown by the dashed line. The location of an edge corresponds to finding a change of sign in the response curve of the receptive field. Such a point is called a zero crossing and its detection leads to the location of the edge in the image.

can be approximated by the difference-of-Gaussians (DOG) function[12]:

$$\nabla^2 G(x, y) \cong \left[\frac{1}{(2\pi)^{1/2} \sigma_e} \exp\left(\frac{-\Delta x^2 + \Delta y^2}{2\sigma_e^{\,2}} \right) \right] - \left[\frac{1}{(2\pi)^{1/2} \sigma_i} \exp\left(\frac{(-\Delta x^2 + \Delta y^2)}{2\sigma_i^{\,2}} \right) \right] \quad (2)$$

where σ_e is the standard deviation of the central excitatory cell distribution, σ_i is the standard deviation of the larger inhibitory cell distribution, and the Δx and Δy coordinates reference the center of the cell ($\Delta x = \Delta y = 0$ at center). Optimal edge discrimination is achieved when $\sigma_i = 1.6\,\sigma_e$ (Ref. 11), and this ratio was used to generate the one- and two-dimensional plots shown in Fig. 3.

Of equal importance in understanding the functioning of the X-cell is the integral of the response of the combined excitatory and inhibitory cells (see Fig. 3). If the entire cell ensemble is under either constant illumination or no illumination, the excitatory and inhibitory sections combine to yield a null response, and thus no signal is generated by the ganglion network. In contrast, a discontinuity in light intensity within the cell boundaries will produce a signal. A maximum signal will be achieved for a centered ($\Delta x = \Delta y = 0$) point source. Thus, the X-cell is most sensitive to edges. Less obvious is the response of the X-cell to motion. If an object illuminates the cell while simultaneously moving across the cell, the edge detection characteristics will respond to that motion with enhanced sensitivity. A motion-enhanced response is due to the fact that the maximum signal is 'remembered' by the ganglion network, and motion will probably enhance the signal during the neural integration time (~ 0.02s). Thus, the X-cell provides both edge and motion discrimination.

Although the X-cell is the most numerous cell type, many different types populate the mammalian retina. The X-cell architecture is particularly relevant to the present discussion because the basic features of this cell can be exploited directly by using orientated bacteriorhodopsin.

Protein-based artificial retinas

An artificial retina may be defined as one that mimics the image-discriminating capabilities of the neural system of the retina. At this stage, most research is not directed towards the development of artificial eyes to replace non-functioning human eyes but, rather, imaging systems that mimic the functionality of the neural system in the retina. This goal must be accomplished before the far more ambitious goal of achieving biomedically relevant implants can be addressed.

There are two types of bacteriorhodopsin-based artificial retinas that are currently being studied. The

Figure 4

A thin film of orientated bacteriorhodopsin enclosed between two optically transparent conducting plates (**a**) generates a differential responsivity when illuminated (**b**). When the light is first turned on, a photocurrent is generated due to the proton-pumping process. The photocurrent reaches saturation within 1–2 ms following illumination and then returns to zero with a time constant of ~30 ms – in this example (these times are variable, and depend upon protein concentration, film thickness and light intensity). The photocurrent self-stabilizes at zero until the light is turned off, at which time a current pulse of identical shape but opposite polarity is generated. Thus, the light sensor responds to differential light intensity. The bipolar response can be used to indicate the direction of the change, or the current output can be rectified if motion or edge detection is the principal concern. Abbreviation: ITO, indium–tin–oxide.

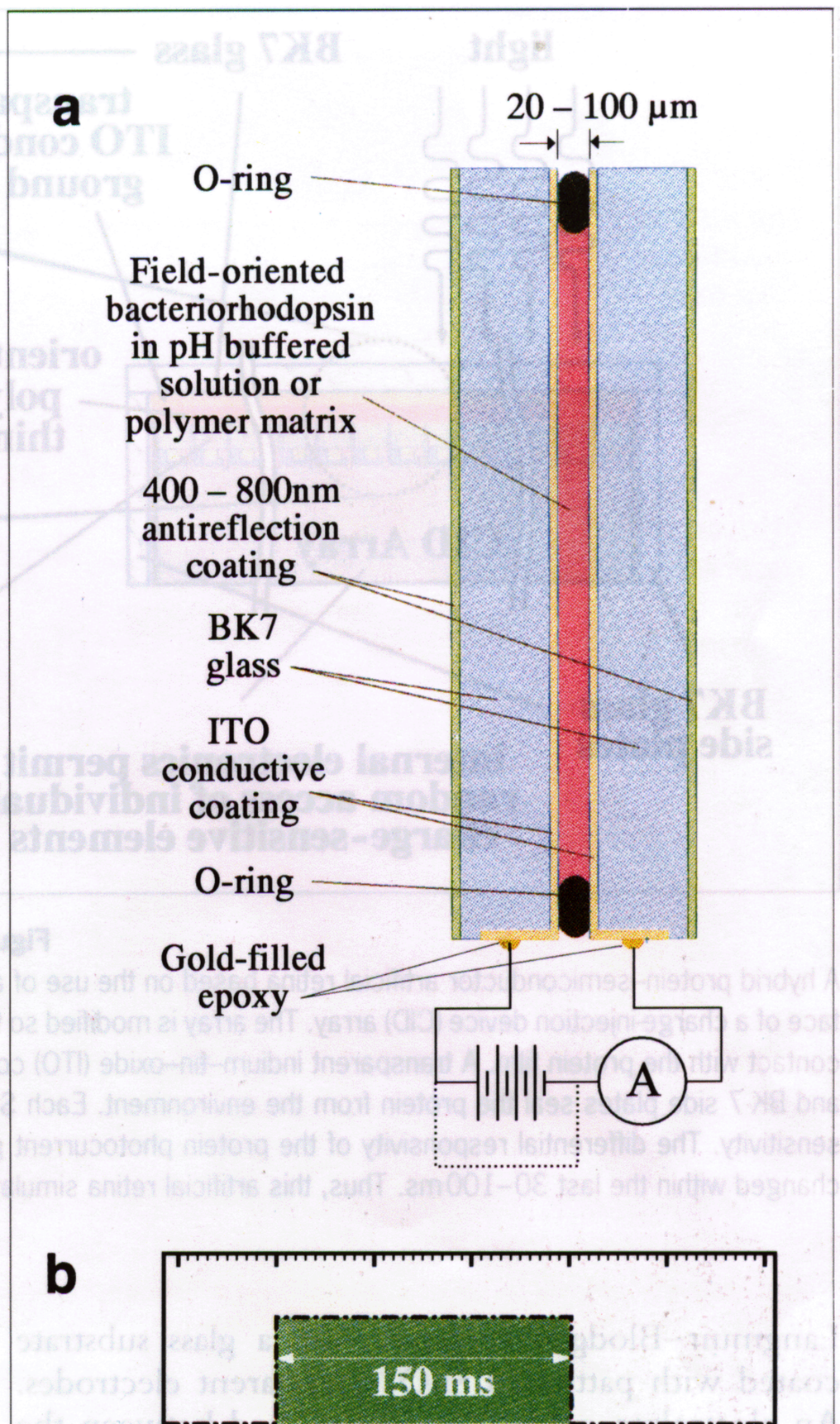

first type uses the differential responsivity of orientated bacteriorhodopsin[7,8,13–16] to create a differentially enhanced image. The second implements a pseudo X-cell architecture by using etching or optical lithography to produce excitatory and inhibitory regions[17,18]. Both designs offer edge enhancement and motion detection. The former offers simplicity of design and high resolution; the latter offers higher speed and the implementation of designs that more closely mimic actual retina performance.

Differential-responsivity imaging systems

The key elements required for observing differential responsivity in bacteriorhodopsin are shown in Fig. 4 (Refs 7,8,13–16). A thin film of bacteriorhodopsin in solution or in a polymer matrix is compressed between two transparent, conducting electrodes. An external field is applied to orientate the protein and, in many cases, the voltage is maintained to provide a current source. The protein responds to light by translocating a proton, and this proton-pumping process generates an electric current. The photocurrent reaches saturation within 1–2 ms following illumination and then returns to zero with a time constant of ~30 ms in the example shown in Fig. 4. The photocurrent self-stabilizes at zero until the light is turned off, at which time a current pulse of identical shape but opposite polarity is generated. Thus, the light sensor responds to differential light intensity rather than to absolute light intensity. Although there is no consensus in the literature regarding the physical origin of the differential responsivity, the following mechanism represents a realistic possibility. Upon the absorption of light, the proton-pumping process generates a current due to ion motion but, eventually, the light-induced ion motion is balanced by leakage in the opposite direction. As the ion distribution reaches a steady-state differential, the current drops back to zero and stays at zero until the light is turned off. The resulting 'off signal' is associated with the back current generated by the motion of ions in the opposite direction from the light-induced translocation. The back current is driven by thermodynamics and lowers the energy of the system by achieving a homogeneous distribution (or zero gradient) of ions.

One of the first imaging devices constructed by using the differential responsivity of bacteriorhodopsin was reported recently by Miyasaka *et al.*[13]. These investigators implemented an artificial photoreceptor with 8×8 (=64) pixels. The device consists of a thin film of bacteriorhodopsin that is orientated by the

 0167 – 7799/93/$6.00

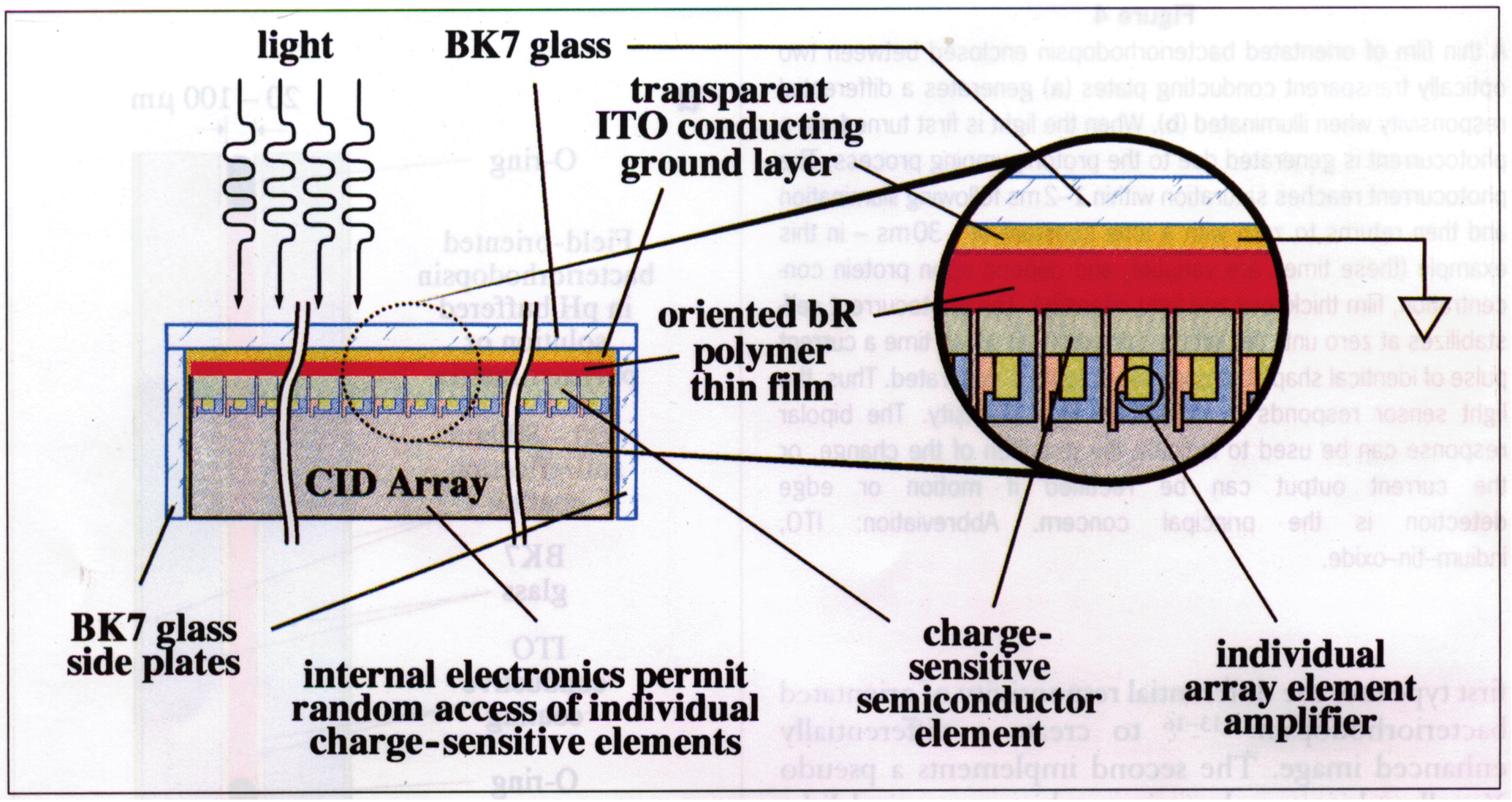

Figure 5

A hybrid protein–semiconductor artificial retina based on the use of a thin film of oriented bacteriorhodopsin deposited directly on the surface of a charge-injection device (CID) array. The array is modified so that the charge-sensitive semi-conductor elements (SCCE) are in direct contact with the protein film. A transparent indium–tin–oxide (ITO) conductive coating on BK-7 glass is placed over the top, and this glass and BK-7 side plates seal the protein from the environment. Each SCCE has an individual amplifier that provides 100 photons pixel^{-1} s^{-1} sensitivity. The differential responsivity of the protein photocurrent generates a final image that is selective of those elements that have changed within the last 30–100 ms. Thus, this artificial retina simulates the motion-sensitive characteristics of its biological counterpart.

Langmuir–Blodgett technique on a glass substrate coated with patterned SnO_2 transparent electrodes. An electrolyte gel is then sandwiched between the protein film and a gold-coated glass plate. Irradiating the bR film causes current to flow in an external circuit connected to the two electrodes. Because of the differential responsivity of the bacteriorhodopsin thin film, the pixels do not generate a signal under constant illumination, but only in response to changes in illumination[13].

The 8×8 imaging array of Miyasaka and co-workers connects each individual pixel to an external amplifier/detector circuit. Such an approach provides excellent control over sensitivity and threshold, but would be difficult to implement in densities of more than 400 pixels. An alternative approach under investigation in our laboratory is to use modified charge-injection device (CID) arrays to monitor the bacteriorhodopsin photocurrent (Fig. 5). The CID is an x–y addressable two-dimensional imaging array capable of producing an electrical output that is proportional to the light incident upon each addressed pixel location. Generally, the CID is used as the photon-to-electrical signal converter and, as such, provides a video signal representation of an image formed on the pixel array surface. The approach used here is to use the x–y addressibility of the CID as a two-dimensional spatial multiplexer to monitor the charge deposited on the CID surface by an orientated layer of bacteriorhodopsin. In other words, the protein provides the light-to-voltage conversion and the CID spatially samples the protein-induced photocurrent at discrete sites by applying an appropriate x–y address.

Our preliminary design uses a 256×256 array of charge-sensitive semiconductor elements (CSSEs) with 15 μm spacing between the elements in both dimensions. The passivation layer that is normally placed on top of these elements is replaced by a thin film of bacteriorhodopsin in polyvinyl alcohol photographic gelatin. The protein is field-orientated prior to polymerization. A cover plate consisting of BK7 glass with a transparent conducting indium–tin–oxide (ITO) coating is then placed across the top to seal the protein layer and to provide a conducting ground plane as reference (Fig. 5). Each CSSE pixel monitors surface charge generated as a function of the differential light intensity at the pixel (Fig. 4). The CID array includes an individual amplifier for each pixel that provides ~100 photons pixel^{-1} s^{-1} sensitivity. One problem that remains to be solved is due to cross-talk between neighboring pixels, which decreases the resolution and differential sensitivity of the imaging array. The cross-talk occurs because the thickness of the protein thin-film permits charge to be distributed to more than one CSSE. Were it possible to make the protein thin-film infinitely thin, there would be no cross-talk problem. Accordingly, the goal is to make the protein film as thin as possible while maintaining an optical density of at least 0.4. The thinnest film we have been able to make with this absorptivity has a thickness of ~30 μm but, in principle, a film of ~10 μm thickness should be feasible.

If this project is successful, a number of advantages will accrue due to the use of a protein–semiconduc-

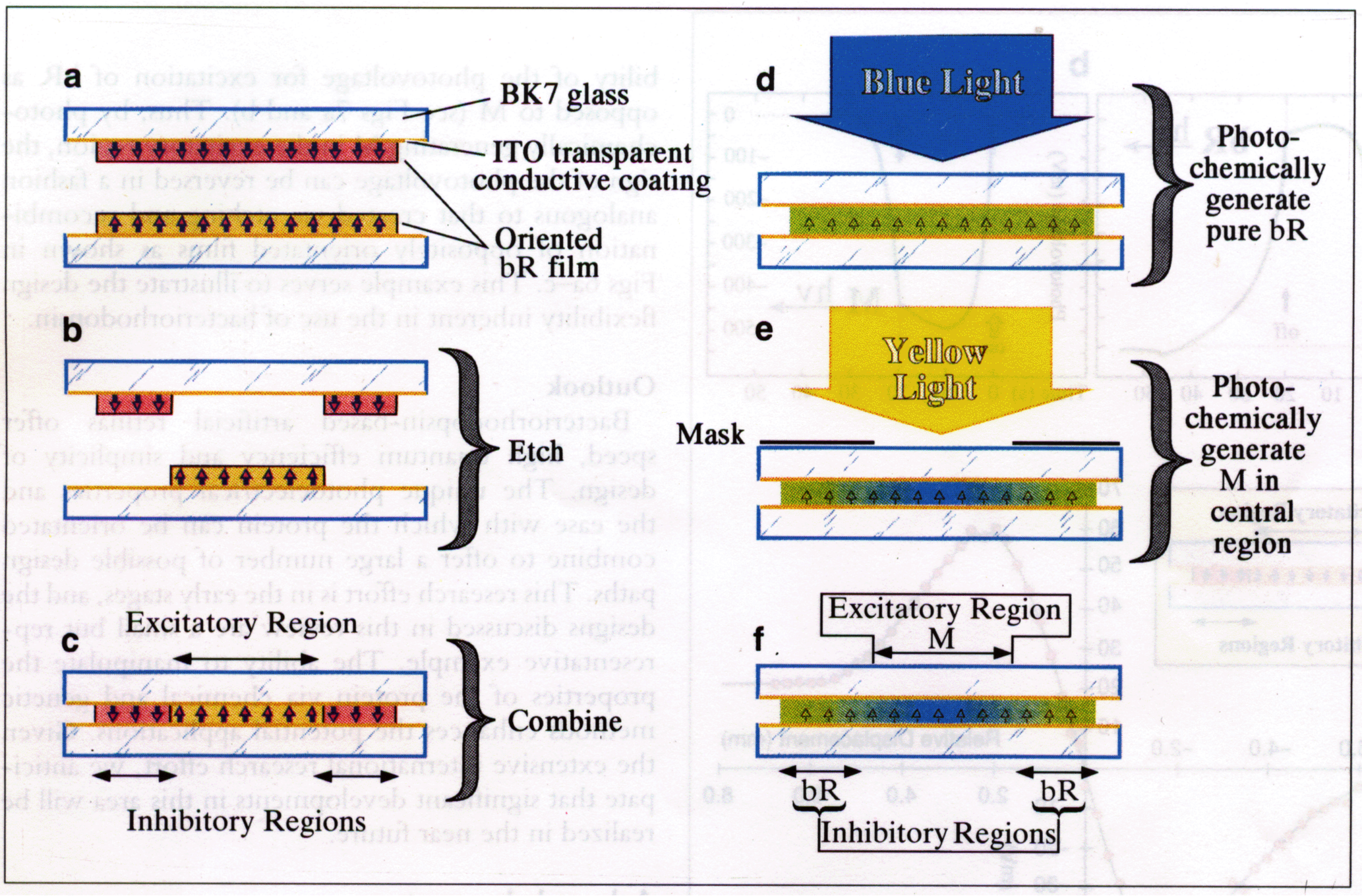

Figure 6

Two methods of simulating an X-cell ganglion receptive field by using the photovoltaic properties of oriented bacteriorhodopsin films. Inserts (**a**)–(**c**) illustrate the use of etched-film techniques to create the excitatory and inhibitory regions. The purple membrane is first oriented on a glass substrate with a transparent, conducting indium–tin–oxide (ITO) film using electrophoresis (**a**). Excitatory and inhibitory regions are then patterned on the two separate films and appropriate sections are removed from each film by laser ablation (**b**). These two films are then oriented face to face and brought into contact (**c**). The molecules in the center region are oriented in a direction opposite to that of the surrounding region. The photovoltage generated by the protein in the center area is positive and represents the excitatory region, while the photovoltage from the surrounding area is opposite in polarity and represents the inhibitory region. Inserts (**d**)–(**f**) illustrate the procedure of producing the receptive field by using the bipolar photoresponse of an oriented film. This film is prepared as in (**a**) and is illuminated with blue light ($400\,nm < \lambda < 480\,nm$) to reset all molecules to the bR state. Then a mask is placed over the film and the central excitatory region is exposed to yellow light ($550\,nm < \lambda < 650\,nm$), which converts ~70% of the molecules to the M state. When white image light reaches such a detector, irradiation of molecules in the bR state will produce a voltage signal that is oppositely polarized from that generated by regions populated primarily by molecules in the M state. The response curve of an X-cell receptive field can be simulated accurately by fine tuning the photochemical lithography (see text).

tor hybrid approach. One of the key characteristics of the internal electronics of the CID array is the ability to access randomly the individual charge-sensitive elements or to read the entire image as a data stream. (Random access is unique to the CID array and differentiates it from CCD arrays.) Accordingly, software can be developed that monitors an entire image, selects those portions of the image exhibiting differential light intensities (i.e. indicate moving objects), and then selectively monitor the 'interesting' portions of the image. Note that a complex but static background will appear black to such a detector array. Therein lie the advantages for robotic-vision applications.

Protein-based X-cell architectures

Although the differential responsivity of bacteriorhodopsin offers a direct application of edge- and motion-enhanced imaging, this approach does not mimic exactly the excitatory and inhibitory processes inherent in the ganglion cells of the retina (Fig. 3). As shown in Fig. 6, the unusual photoelectric properties of orientated bacteriorhodopsin can be used to implement artificial photoreceptors that mimic the ganglion receptive field. Two methods of preparing the artificial photoreceptor cells have been investigated, one based on etching (Figs 6a–c) and one based on photochemical lithography (Figs 6d–f; Ref. 18). The response of artificial photoreceptors prepared by etching to a sharp edge of light is shown in Fig. 7.

The mechanism of the etched imaging cell (Figs 6a–c) is simple. An orientated thin film of bacteriorhodopsin will produce a photoelectric signal with a polarity that is determined by the orientation of the protein. If two identically orientated films are etched and combined as shown in Figs 6a–c, irradiation of the central region will produce a photovoltage that is opposite to that of the circular outer region because the regions have opposite protein orientation. Note that, in both areas, the bR $\rightarrow$ M photochemical reaction is responsible for the photovoltage, and a low photoconversion rate will ensure linearity of response[17,18]. The use of laser ablation to etch the

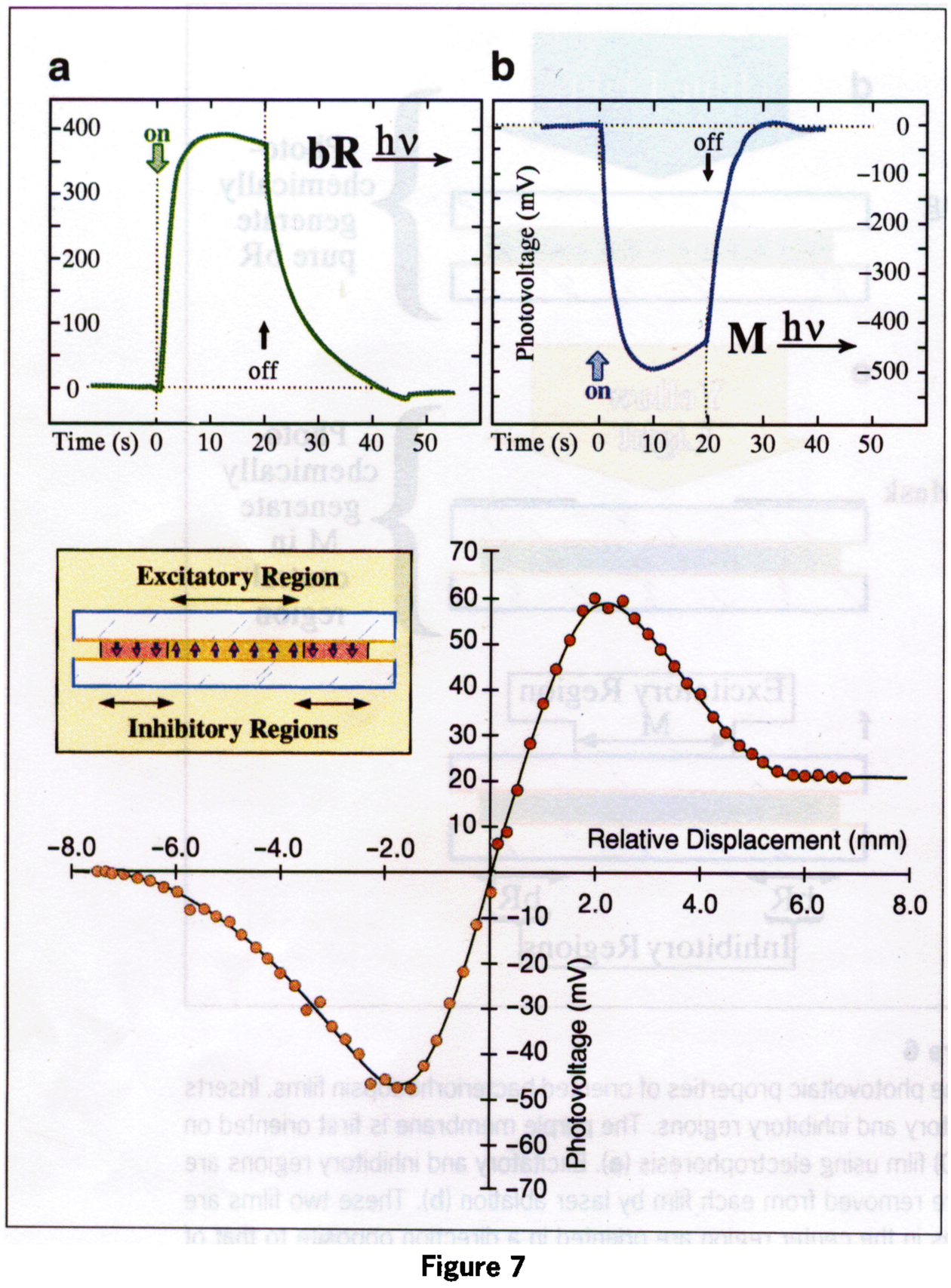

Figure 7

The bipolar response of an oriented bacteriorhodopsin film is shown for the forward and reverse photoreactions in (**a**) and (**b**), and the response characteristics of an edge detector constructed following the methods and procedures outlined in Fig. 6a–c is shown in (**c**). The photovoltages in (**a**) and (**b**) were measured by using yellow light and blue light excitation, respectively. The photovoltage in (**c**) was measured as a function of edge position of a white light source scanned across the cell. The experimental data are indicated by filled circles and the solid line is a smoothed representation of the data. The horizontal axis corresponds to the relative displacement between the edge and the center of the receptor field. A zero crossing is detected when the position of the sharp edge coincides with the center of the receptive field. Note that the observed response is very similar to the integral curve shown in Fig. 3a. (Adapted from Ref. 17.)

elements permits very small cell architectures. The response of the artificial receptor cell is shown in Fig. 7c, and closely mimics the response of the ganglion X-cell receptive field shown in Fig. 3.

The alternative approach based on photochemical lithography (Figs 6d–f) is more easily implemented, but generates a transient receptor cell that must be continuously regenerated photochemically. However, such a design offers flexibility in implementing a variety of receptive fields with different characteristics. By using back illumination, a blue:yellow filter mask and two colored light sources ($400 < \lambda < 420$ nm and $550 < \lambda < 600$ nm), an imaging system can be constructed with variable response characteristics. We introduce it here primarily for the purposes of illustration. The key physical property of the protein that is used in implementing this artificial receptor cell is the reversibility of the photovoltage for excitation of bR as opposed to M (see Figs 7a and b). Thus, by photochemically generating M in the excitatory region, the sign of the photovoltage can be reversed in a fashion analogous to that created via etching and recombination of oppositely orientated films as shown in Figs 6a–c. This example serves to illustrate the design flexibility inherent in the use of bacteriorhodopsin.

Outlook

Bacteriorhodopsin-based artificial retinas offer speed, high quantum efficiency and simplicity of design. The unique photoelectrical properties and the ease with which the protein can be orientated combine to offer a large number of possible design paths. This research effort is in the early stages, and the designs discussed in this review are a small but representative example. The ability to manipulate the properties of the protein via chemical and genetic methods enhances the potential applications. Given the extensive international research effort, we anticipate that significant developments in this area will be realized in the near future.

Acknowledgements

Research from the authors' laboratory was sponsored, in part, by grants from the W. M. Keck Foundation, the National Institutes of Health, Biological Components Corp., CID Technologies Inc. and the New York State Center for Advanced Technology in Computer Applications and Software Engineering.

References

1 Mahowald, M. A. and Mead, C. (1991) *Sci. Am.* May, 76–82
2 Oesterhelt, D. and Stoeckenius, W. (1971) *Nature N. Biol.* 233, 149–152
3 Birge, R. R. (1990) *Biochim. Biophys. Acta* 1016, 293–327
4 Oesterhelt, D., Brauchle, C. and Hampp, N. (1991) *Quart. Rev. Biophys.* 24, 425–478
5 Birge, R. R., Masthay, M. B., Stuart, J. A., Tallent, J. R. and Zhang, C. F. (1991) *Proc. SPIE* 1432, 129–140
6 Hayward, B. S., Grano, D. A., Glaeser, R. M. and Fisher, K. A. (1978) *Proc. Natl Acad. Sci. USA* 75, 4320–4324
7 Birge, R. R. (1990) *Annu. Rev. Phys. Chem.* 41, 683–733
8 Birge, R. R. (1992) *IEEE Computer* 25, 56–67
9 Earnest, T. N., Roepe, P., Braiman, M. S., Gillespie, J. and Rothschild, K. J. (1986) *Biochemistry* 25, 7793–7798
10 Birge, R. R., Zhang, C. F. and Lawrence, A. F. (1989) in *Molecular Electronics* (Hong, F., ed.), pp. 369–379, Plenum Press
11 Lennie, P., Trevarthen, C., Van Essen, D. and Wässle, H. (1990) in *Visual Perception. The Neurophysiological Foundations* (Spillmann, L. and Werner, J. S., eds), pp. 103–128, Academic Press
12 Marr, D. and Hildreth, E. (1980) *Proc. R. Soc. London Ser. B* 207, 187–217
13 Miyasaka, T., Koyama, K. and Itoh, I. (1992) *Science* 255, 342–344
14 Sasabe, H., Furuno, T. and Wada, T. (1988) *Mol. Cryst. Liq. Cryst.* 160, 281–296
15 Sasabe, H., Furuno, T. and Takimoto, K. (1989) *Synthetic Metals* 28, C787–C792
16 Sasabe, H., Furuno, T. and Ulmer, K. M. (1989) in *Molecular Electronics – Science and Technology* (Aviram, A., ed.), pp. 285–292, Engineering Foundation, New York
17 Chen, Z., Takei, H. and Lewis, A. (1990) *Proc. Int Joint Conf. Neural Networks* 2, 803–807
18 Takei, H., Lewis, A., Chen, Z. and Nebenzahl, I. (1992) *Applied Optics* 30, 500–509